

### 3 Numerical Methods for Convection

The topic of computational fluid dynamics (CFD) could easily occupy an entire semester – indeed, we have such courses in our catalog. The objective here is to examine some of the basic features of solving, via numerical means, the DEs which describe convective–diffusive transport. We will restrict the analysis to 2–D, laminar, and incompressible problems. The notes will not describe, in any depth, topics that are commonly dealt with in a numerical methods course – i.e., solution of ODEs and solution of linear equations – and which can be implemented using the black box routines in matlab or mathematica. Rather, we will concentrate on the issues involved in casting the DEs into a numerical form.

#### 3.1 The stream function–vorticity formulation

The incompressible continuity and momentum equations appear as

$$\nabla \cdot \mathbf{u} = 0 \quad (1)$$

$$\frac{D\mathbf{u}}{Dt} = -\frac{1}{\rho} \nabla P + \nu \nabla^2 \mathbf{u} + \frac{\mathbf{f}}{\rho} \quad (2)$$

in which  $\nabla^2$  represents, in this case, the *vector Laplacian*:

$$\nabla^2 \mathbf{u} = \underbrace{\nabla(\nabla \cdot \mathbf{u})}_{=0} - \nabla \times \nabla \times \mathbf{u} \quad (3)$$

in which the incompressible continuity equation was applied.

Together, these equations represent  $S+1$  equations, where  $S$  is the spacial dimension of the problem (i.e., 1–D, 2–D, etc.). Unknowns are the  $S$  components of the velocity  $\mathbf{u}$  and the pressure  $P$ ; these are sometimes known as the *primitive variables* to the problem. Obtaining a solution in primitive variables is challenging, in large part due to the nature of the pressure dependence on the problem. Observe that the pressure appears only in the gradient operator, and in this sense nowhere – for this incompressible model – does the absolute value of the pressure affect the problem. That is,  $P + C$ , where  $C$  is an arbitrary constant, will always satisfy the incompressible momentum equations. The fact that the pressure appears in a first–order spacial derivative also make difficult the specification of boundary conditions for the pressure: one can not arbitrarily set values of pressure on all the boundaries, as this will overconstrain the problem.

Often the pressure field is not of interest in itself. For such cases the pressure can be eliminated from the problem by introduction of the *vorticity* vector  $\boldsymbol{\omega}$ . The vorticity is defined as the curl of the velocity;

$$\boldsymbol{\omega} = \nabla \times \mathbf{u} \quad (4)$$

The vorticity transport equation is obtained by taking the curl of the momentum equation. Since the curl of the gradient of any scalar is always zero, i.e.,

$$\nabla \times \nabla P = 0 \quad (5)$$

the pressure field is identically eliminated from the resulting equation. The convective part in the material derivative can be reduced by using the vector identity:

$$(\mathbf{u} \cdot \nabla) \mathbf{u} = \frac{1}{2} \nabla(\mathbf{u} \cdot \mathbf{u}) - \mathbf{u} \times \nabla \times \mathbf{u} = \frac{1}{2} \nabla(\mathbf{u} \cdot \mathbf{u}) - \mathbf{u} \times \boldsymbol{\omega} \quad (6)$$

and since the curl of a gradient is identically zero, the first term is eliminated when the curl of the momentum equation is taken. Using Eq. (3), the curl of  $\nabla^2 \mathbf{u}$  will equal  $\nabla^2 \boldsymbol{\omega}$ , because the divergence of a curl is also identically zero. Therefore, the *vorticity transport equation* for an incompressible fluid appears as

$$\frac{\partial \boldsymbol{\omega}}{\partial t} - \nabla \times (\mathbf{u} \times \boldsymbol{\omega}) = \nu \nabla^2 \boldsymbol{\omega} + \frac{1}{\rho} \nabla \times \mathbf{f} \quad (7)$$

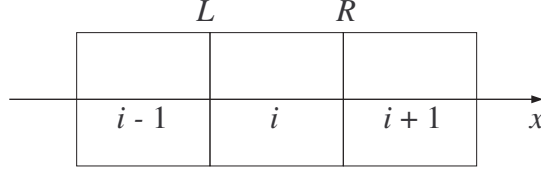


Figure 1: Control volume

One more vector identity is now used:

$$\nabla \times (\mathbf{u} \times \boldsymbol{\omega}) = (\boldsymbol{\omega} \cdot \nabla) \mathbf{u} - (\mathbf{u} \cdot \nabla) \boldsymbol{\omega} - \underbrace{\boldsymbol{\omega}(\nabla \cdot \mathbf{u})}_{=0} + \underbrace{\mathbf{u}(\nabla \cdot \boldsymbol{\omega})}_{=0} \quad (8)$$

and using the definition of the material derivative;

$$\frac{D\boldsymbol{\omega}}{Dt} = (\boldsymbol{\omega} \cdot \nabla) \mathbf{u} + \nu \nabla^2 \boldsymbol{\omega} + \frac{1}{\rho} \nabla \times \mathbf{f} \quad (9)$$

Note that the velocity field still appears in the vorticity transport equation by virtue of the material derivative, i.e.,

$$\frac{D}{Dt} = \frac{\partial}{\partial t} + \mathbf{u} \cdot \nabla \quad (10)$$

Everything appearing up to this point is for a general, 3-D incompressible flow. We now restrict our model to the 2-D cartesian case. The vorticity can now be treated as a scalar, since for 2-D  $x, y$  coordinates  $\boldsymbol{\omega}$  will point only in the  $z$  direction. The first term on the right hand side of Eq. (9) will also be zero for the 2-D case, since  $\boldsymbol{\omega} \cdot \nabla = \omega \partial/\partial z$ . The continuity equation can be identically satisfied by use of the stream function  $\psi$ , for which

$$u = \frac{\partial \psi}{\partial y}, \quad v = -\frac{\partial \psi}{\partial x} \quad (11)$$

Equation (4) will become

$$\frac{\partial^2 \psi}{\partial x^2} + \frac{\partial^2 \psi}{\partial y^2} = -\omega \quad (12)$$

And Eq. (9) is

$$\frac{d\omega}{dt} + \frac{\partial(u\omega)}{\partial x} + \frac{\partial(v\omega)}{\partial y} = \nu \left( \frac{\partial^2 \omega}{\partial x^2} + \frac{\partial^2 \omega}{\partial y^2} \right) + \frac{1}{\rho} \left( \frac{\partial f_y}{\partial x} - \frac{\partial f_x}{\partial y} \right) \quad (13)$$

in which the velocity components are implicitly understood to be obtained from the stream function. Note that the left hand side of Eq. (13) appears in the *divergent* form, whereas Eq. (9) is in the *conservative* form. These forms are equivalent by virtue of the continuity equation (you should prove this to yourself); it turns out that the divergent form will be better suited for numerical computations. For a given body force function  $\mathbf{f}$ , the above two equations represent a set of coupled, nonlinear PDEs for the scalars  $\psi$  and  $\omega$ .

### 3.2 Upwind finite difference scheme

Numerical solution of Eqs. (12) and (13) will typically involve an iteration scheme, the steps of which are 1) Eq. (12) is solved for  $\psi$  using a fixed  $\omega$  field; 2) the velocity components are calculated from  $\psi$ ; 3) Eq. (13) is solved for  $\omega$ ; and 4) the process is repeated until convergence is attained. A *stable* numerical scheme – i.e., one which does converge – will require a special approach to representing the convection terms in Eq. (13), and a typical method is known as the *upwind scheme*.

This approach is best illustrated by simplifying the problem to 1-D, for which the vorticity equation, suitably nondimensionalized, would appear as

$$\frac{\partial \omega}{\partial t} + \frac{\partial(u\omega)}{\partial x} = \frac{1}{Re} \frac{\partial^2 \omega}{\partial x^2} \quad (14)$$

It is implicitly understood that all quantities are dimensionless, i.e.,  $\omega \rightarrow \omega L_c / u_c$ ,  $x \rightarrow x / L_c$ , and  $t \rightarrow t u_c / L_c$ , where  $u_c$  and  $L_c$  are the characteristic velocity and length of the problem and  $Re = u_c L_c / \nu$ .

Now represent the 1-D system as a set of  $N$  control volumes, each of length  $\Delta x$  as illustrated in Fig. (1). It will be assumed that, at some time  $t = k\Delta t$ ,  $\omega$  is uniform within each control volume at some value  $\omega_i^k$ , in which subscript  $i$  denotes the spacial location of the control volume and superscript  $k$  denotes the time step. Per the control volume approach the equation is integrated over the volume of control volume  $i$  and over a single time step. The first term will give the net accumulation of  $\omega$  in the CV during the time step;

$$\text{accumulation} = (\omega_i^{k+1} - \omega_i^k) \Delta x \quad (15)$$

The third term, which represents the diffusive transport of  $\omega$ , will result in the usual central difference approximation of the second derivative. For now we will not specify whether  $\omega$  will be evaluated at the current time step  $k$ , or at  $k+1$ , or some average;

$$\text{diffusion} = (\omega_{i+1} + \omega_{i-1} - 2\omega_i) \frac{\Delta t}{Re \Delta x} \quad (16)$$

The most problematic evaluation, insofar as numerical methods are concerned, is that for the convective transport term. The integration gives

$$\text{convection} = (u_R \omega_R - u_L \omega_L) \Delta t \quad (17)$$

in which  $L$  and  $R$  denote the values on the boundaries of the control volume. For this 1-D case, the values of  $u_L$  and  $u_R$  could be approximated as the average of the  $u$  values in the neighboring control volumes, i.e.,  $u_L = (u_{i-1} + u_i)/2$ . The choice of  $\omega_L$  and  $\omega_R$  is less obvious. If  $u$  is positive, meaning that the flow is going from left to right, the value of  $\omega$  at the left boundary would likely be weighted more towards  $\omega_{i-1}$  than  $\omega_i$ , and that at the right boundary would also be closer to  $\omega_i$  than  $\omega_{i+1}$ . In other words, the value of  $\omega$  at the boundary will be pushed towards that in the *upwind* direction. Including this simple effect into the numerical scheme is actually critical to insure an accurate and stable solution. The most simple approach, which is used here, is the upwind scheme: the value of  $\omega$  at the boundary is set equal to that for the upwind CV. The upwind direction depends only on the sign of  $u$ , and by use of the absolute value function, the discretized convection term can be written as

$$\text{convection} = [(u_R - |u_R|)\omega_{i+1} + (u_R + |u_R| - u_L + |u_L|)\omega_i - (u_L + |u_L|)\omega_{i-1}] \frac{\Delta t}{2} \quad (18)$$

Observe that half the terms in this equation will always cancel out, depending on the sign of  $u_L$  and  $u_R$ .

This 1-D case is instructive yet not especially challenging: the velocity field for the incompressible 1-D problem will be a constant. The scheme can, however, be extended directly to 2-D without any complication. Take the CV to have dimensions  $\Delta x$ ,  $\Delta y$ , and denote the value of  $\omega$  in the control volume as  $\omega_{i,j}^k$  where  $i$  and  $j$  are the  $x$  and  $y$  position indices. The schematic is illustrated in Fig. (2), for the specific case of  $\Delta x = \Delta y$ . At this point a choice on the time integration method can also be made. In the *explicit* method, the diffusion and convection terms are evaluated at the current time step  $k$ , and the resulting difference scheme will appear as

$$\omega_{i,j}^{k+1} = a \omega_{i+1,j}^k + b \omega_{i-1,j}^k + c \omega_{i,j+1}^k + d \omega_{i,j-1}^k + e \omega_{i,j}^k + \Delta t S_{i,j}^k \quad (19)$$

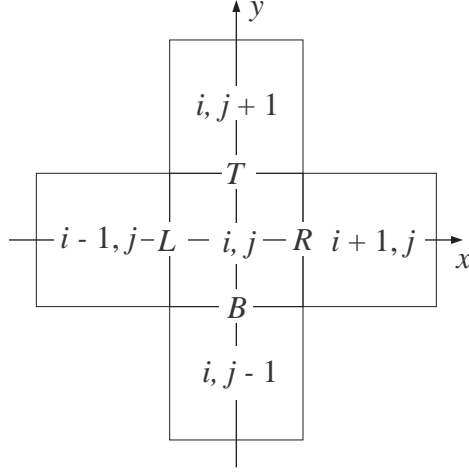


Figure 2: 2-D Control volume

with

$$\begin{aligned}
 a &= \Delta t \left[ \frac{1}{Re(\Delta x)^2} - \frac{1}{2\Delta x}(u_R - |u_R|) \right] \\
 b &= \Delta t \left[ \frac{1}{Re(\Delta x)^2} + \frac{1}{2\Delta x}(u_L + |u_L|) \right] \\
 c &= \Delta t \left[ \frac{1}{Re(\Delta y)^2} - \frac{1}{2\Delta y}(v_T - |v_T|) \right] \\
 d &= \Delta t \left[ \frac{1}{Re(\Delta y)^2} + \frac{1}{2\Delta y}(v_B + |v_B|) \right] \\
 e &= 1 - \Delta t \left[ \frac{2}{Re(\Delta x)^2} + \frac{2}{Re(\Delta y)^2} + \frac{1}{2\Delta x}(u_R + |u_R| - u_L + |u_L|) + \frac{1}{2\Delta y}(v_T + |v_T| - v_B + |v_B|) \right]
 \end{aligned} \tag{20}$$

The quantity  $S_{i,j}^k$  in Eq. (19) represents a source term, which typically arises due to natural convection. Subscripts  $T$ ,  $B$ ,  $R$ , and  $L$  denote the top, bottom, right, and left faces of the CV.

Equation (19) represents an explicit equation for the value of  $\omega_{i,j}^{k+1}$  as a function of the field values at step  $k$ . Explicit schemes are simple to program and they are first-order accurate in time (i.e., the error scales with  $\Delta t$ ), yet they are stable only for a sufficiently small time step size  $\Delta t$ . The step size criterion is that the coefficient  $e$  in Eq. (20) must be positive. Note that the term in square brackets, in the formula for  $e$ , will always be positive (convince yourself of this by setting the velocities to either positive or negative values). This term, when multiplied by  $\Delta t$ , must therefore be less than unity, and a small spacial grid will therefore require a correspondingly small time step for stability.

The velocity field is obtained from the stream function via Eq. (11). A central difference approximation can be used, so that

$$u_{i,j} = \frac{\psi_{i,j+1} - \psi_{i,j-1}}{2\Delta y}, \quad v_{i,j} = -\frac{\psi_{i+1,j} - \psi_{i-1,j}}{2\Delta x} \tag{21}$$

The finite difference approximation of Eq. (12) appears as

$$\frac{1}{\Delta x} (\psi_{i+1,j} + \psi_{i-1,j} - 2\psi_{i,j}) + \frac{1}{\Delta y} (\psi_{i,j+1} + \psi_{i,j-1} - 2\psi_{i,j}) = -\omega_{i,j} \Delta x \Delta y \tag{22}$$

with all quantities evaluated at time step  $k$ .

### 3.3 The energy equation

The energy equation will have exactly the same form as the  $\omega$  transport equation for the 2-D model. Assuming there is no volumetric source of heat, the energy equation will appear as

$$\frac{dT}{dt} + \frac{\partial(uT)}{\partial x} + \frac{\partial(vT)}{\partial y} = \alpha \left( \frac{\partial^2 T}{\partial x^2} + \frac{\partial^2 T}{\partial y^2} \right) \quad (23)$$

The same issues with regard to discretization of the convection term apply to the energy equation, and an upwind scheme is often used to provide stability. The numerical model of the energy equation will therefore appear as Eq. (19), except with  $\omega$  replaced with  $T$  and  $Re$  replaced with  $Pr Re$ . The source term in Eq. (13) typically occurs as a result of free convection. Under the Boussinesq approximation, and assuming that gravity points in the  $-y$  direction, the body force terms are

$$\frac{f_y}{\rho} = g \beta (T - T_\infty), \quad \frac{f_x}{\rho} = 0 \quad (24)$$

and the dimensionless source term would be

$$S = \frac{g \beta \Delta T_c L_c}{u_c^2} \frac{\partial T}{\partial x} \quad (25)$$

in which  $\Delta T_c$ ,  $L_c$ , and  $u_c$  denote the characteristic temperature difference, length scale, and velocity used to make the problem dimensionless, and  $T$  and  $x$  now denote the dimensionless temperature and length. Note that in free convection problems,  $u_c$  can be set according to

$$u_c = (g \beta \Delta T_c L_c)^{1/2} \quad (26)$$

which results in the Reynolds number in Eqs. (20) being replaced by the square root of the Grashof number.

The source term in Eq. (19) can be obtained by applying a central difference approximation to Eq. (25), i.e.,

$$S_{i,j} = \frac{g \beta \Delta T_c L_c}{u_c^2} \frac{T_{i+1,j} - T_{i-1,j}}{2\Delta x} \quad (27)$$

### 3.4 Boundary conditions

Full closure of the numerical model for  $\omega$  and  $\psi$  in Eqs. (19) and (22) requires specification of boundary conditions. Often the boundary conditions are not obvious, especially in the case where the boundary of the *numerical domain* is not an actual physical boundary. For example, a simulation of boundary layer flow requires that one boundary (say at  $x = L$ ) correspond to an inflow condition, and the opposite boundary ( $x = 0$ ) represent an outflow. The inflow conditions may be identifiable (say uniform  $u = u_\infty$ ), yet the outflow conditions are not obvious. In general, we (i.e., the observers of the physical event) do not have control of the conditions at the outflow: such conditions depend on what happens inside the system. In this sense, a modeling of the outflow conditions requires some assumption regarding the nature of the flow, i.e., fully developed, isothermal, etc.

Table 12.1 of Bejan lists the common formulation of the boundary conditions on streamfunction, vorticity, and temperature. This table is reproduced on the following page. The formulations in the table correspond to a mesh that places the nodes of the control volumes directly on the surfaces. This approach works best when the boundary condition corresponds to a fixed value of the variable, i.e.,  $T = T_s$  on the surface. It is also possible to place the boundary of the control volume on the surface; such an approach is better suited for specified flux conditions.

**Table 12.1 Boundary Conditions for Streamfunction, Vorticity, and Temperature**

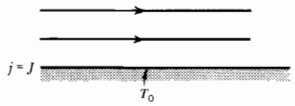
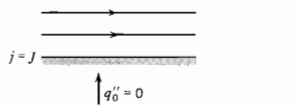
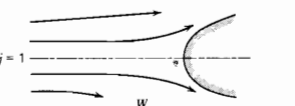

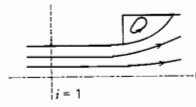
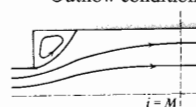
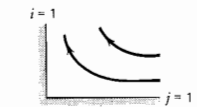
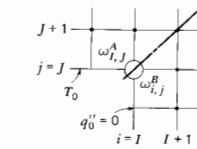
Boundary Description	$\psi$	$\omega$	$T$
<p>Solid impermeable wall; specified wall temperature</p> 	$\psi_{i,J} = 0$	$\omega_{i,J} = \frac{-2(\psi_{i,J+1} - \psi_{i,J})}{(\Delta y)^2}$ <p>or</p> $\omega_{i,J} = \frac{7\psi_{i,J} - 8\psi_{i,J+1} + \psi_{i,J+2}}{2(\Delta y)^2}$	$T_{i,J} = T_0$ or $T_{i,J} = f(x)$
<p>Impermeable and adiabatic wall</p> 	$\psi_{i,J} = 0$	$\omega_{i,J} = \frac{-2(\psi_{i,J+1} - \psi_{i,J})}{(\Delta y)^2}$ <p>or</p> $\omega_{i,J} = \frac{7\psi_{i,J} - 8\psi_{i,J+1} + \psi_{i,J+2}}{2(\Delta y)^2}$	$T_{i,J} = T_{i,J+1}$ or $T_{i,j} = \frac{1}{3}(4T_{i,J+1} - T_{i,J+2})$
<p>Axis of symmetry</p> 	$\psi_{i,1} = 0$	$\omega_{i,1} = 0$	$T_{i,1} = T_{i,2}$
<p>Far field conditions; the velocity <math>U_\infty</math>, temperature <math>T_\infty</math>, and entrainment velocity <math>v_\infty</math> are assumed known.</p> 	$\psi_{i,N} = \int_{y_1}^{y_N} u(y) dy$	$\omega_{i,N} = \frac{2(-\psi_{i,N-1} + \psi_{i,N} - U_\infty \Delta y)}{(\Delta y)^2}$ <p>(<math>v_\infty = 0</math> was assumed)</p>	$T_{i,N} = T_\infty$
<p>Inflow conditions, inflow velocity, and temperature profiles (<math>u, T</math>) are assumed known and <math>v</math> is allowed to develop</p> 	$\psi_{1,j} = \int_{y_j}^{y_N} u(y) dy$	$\omega_{1,j} = -\frac{\partial u}{\partial y}\bigg _{1,j} + \frac{\partial v}{\partial x}\bigg _{1,j}$ $= -\frac{\partial u}{\partial y}\bigg _{1,j} - \frac{\psi_{1,j} + \psi_{3,j} - 2\psi_{2,j}}{(\Delta x)^2}$	$T_{1,j} = T_1$
<p>Outflow conditions</p> 	$\psi_{M,j} = 2\psi_{M-1,j} - \psi_{M-2,j}$	$\omega_{M,j} = \omega_{M-1,j}$	$T_{M,j} = T_{M-1,j}$
<p>Concave sharp corner</p> 	$\psi_{1,1} = 0$	$\omega_{1,1} = 0$	$T_{1,1} = \frac{1}{2}(T_{1,2} + T_{2,1})$
<p>Convex sharp corner</p> 	$\psi_{I,J} = 0$	<p>To calculate <math>\omega_{I,J+1}</math>,</p> $\omega_{I,J}^A = \frac{-2(\psi_{I,J+1} - \psi_{I,J})}{(\Delta y)^2}$ <p>To calculate <math>\omega_{I+1,J}</math>,</p> $\omega_{I,J}^B = \frac{-2(\psi_{I+1,J} - \psi_{I,J})}{(\Delta x)^2}$	<p>To calculate <math>T_{I,J+1}</math>,</p> $T_{I,J}^A = T_0;$ <p>To calculate <math>T_{I+1,J}</math>,</p> $T_{I,J}^B = T_{I+1,J}$

Figure 3: Boundary condition formulations, from Bejan

### 3.5 The explicit algorithm

Everything is in place as far as the numerical model is concerned. The basic algorithm to generating a numerical solution is as follows.

1. Initialize  $\omega_{i,j}^0 = 0$ ,  $T_{i,j}^0 = T_0$ , and set the boundary values for the specified problem.
2. For  $k = 0, 1, \dots$ ,
  - (a) Solve the system of equations for  $\psi$ , Eq. (22), using the current values of  $\omega_{i,j}^k$ .
  - (b) Use the solution for  $\psi_{i,j}$  to calculate the  $u$  and  $v$  velocity components.
  - (c) Calculate the values of  $\omega_{i,j}^{k+1}$  and  $T_{i,j}^{k+1}$  using the explicit scheme, Eq. (19).
  - (d) Check to see if steady-state is reached.
3. Use the solution for  $u$ ,  $v$ , and  $T$  to compute the sought properties, i.e.,  $Nu$ .

This approach provides a relatively slow yet safe route to obtaining the steady-state properties of the system. There are more direct methods to obtain steady-state properties, which involve an iterative scheme between Eqs. (22) and the steady form of Eq. (19) (and the corresponding energy equation, if present).

### 3.6 Application to the external boundary layer

#### 3.6.1 Control volume and boundary conditions

We will plan to apply the basic numerical scheme, described in the previous sections, to predicting surface–fluid transport properties (friction coefficient, Nusselt number) for a variety of flow conditions as we encounter them. The first flow condition examined, that being the laminar external boundary layer, is actually one of the most problematic set up in the numerical model. The difficulty arises from specifying the boundary conditions in the computational domain. The situation is illustrated in Fig. (4). The computational control volume consists of a rectangular region, with length  $1 + X_s$  and height  $H$ . Part of the bottom boundary consists of a starting region, of length  $X_s$ , and the remainder corresponds to a physical surface with zero–slip conditions and a specified uniform temperature. The starting region boundary is a free surface with adiabatic and zero stress conditions: it is basically a length of the upstream region, and it is needed so that we can specify, with some confidence, the inflow conditions on the left face of the control volume. These inflow conditions will correspond to a uniform velocity profile and a uniform temperature. Understand that the effects of the surface on the flow will diffuse some distance upstream; the length of the starting section must be somewhat greater than this diffusion length.

The remaining boundary conditions – those on the top and right faces – are more ambiguous. You might suppose that the top surface represents a constant streamline, corresponding to a impermeable surface (i.e., no net flow through the surface). This, however, would not represent the top surface in an external boundary layer problem – no matter how large the height  $H$  of the control volume. The physical surface brings the flow to a halt, and as a consequence, the fluid is displaced from the surface in the upwards direction. A portion of this displacement *must* exit the CV through the top surface. Another way to see this is to consider that the net mass flow rate into the control volume must be zero. The flow enters the CV with uniform velocity, and since the CV has height  $H$ , the flow in to the CV will be  $1 \cdot H$  per unit width. The flow exiting the CV on the right will have an average velocity less than one; it would be physically impossible, in this external (i.e., unconfined) situation, for the  $x$  component of velocity to exceed, at any point, the inlet velocity. Therefore, the flow rate at the outflow surface will have a value somewhat less than  $H$ . To balance mass, some flow must exit the top surface, and the top surface cannot represent a streamline.

A more realistic alternative is to impose, along the top surface, a uniform  $x$  component of velocity of  $u = 1$ . This does not imply that the  $y$  component is zero, yet it does implicitly assume that the height  $H$  of

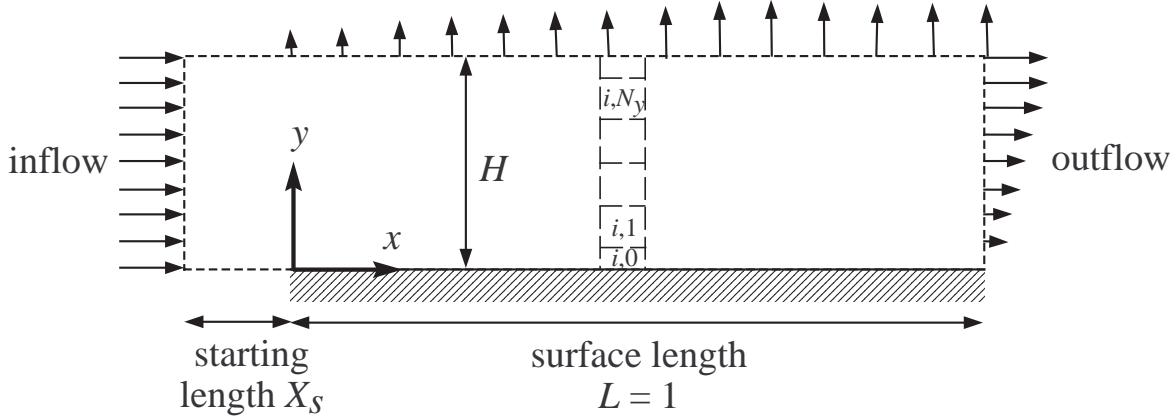


Figure 4: External boundary layer control volume.

the CV is sufficiently large so that the upper surface is in the freestream, i.e., outside of the boundary layer. The uniform  $u$  velocity component at  $y = H$  provide a boundary condition on the streamfunction, and will be described in more detail below.

Of all the CV surfaces, the outflow surface along the right edge has the most contrived boundary conditions. In reality, it would not be possible to accurately specify the conditions at this point, since the conditions will depend on the nature of the flow upstream. The approach used by Bejan for outflow conditions, listed in Fig. (3), is equivalent to

$$\frac{\partial v}{\partial x} = \frac{\partial \omega}{\partial x} = \frac{\partial T}{\partial x} = 0 \quad (28)$$

Again, these are not physically realistic, and in view of this the numerical solution results will be questionable at points near the outflow boundary. However, the outflow conditions will have a relatively small effect on the results near the center of the CV.

### 3.6.2 Discretization

The CV can be divided into a uniform grid of  $N_x + 1$  and  $N_y + 1$  elements in the  $x$  and  $y$  directions. As illustrated in Fig. (4), the boundary elements have half the thickness as the interior elements. The spacial sizes of the elements are

$$\Delta x = \frac{1 + X_s}{N_x}, \quad \Delta y = \frac{H}{N_y} \quad (29)$$

Variables will be labeled with paired subscripts denoting position, i.e.,

$$\psi_{i,j} = \psi(i \Delta x, j \Delta y), \quad i = 0, 1, \dots, N_x; \quad j = 0, 1, \dots, N_y$$

Laminar boundary layer theory (to be discussed eventually!) informs us that the hydrodynamic and thermal boundary layer thicknesses – defined at the points at which the velocity or temperature variable reaches 99% of its free-stream value – vary as

$$\frac{\delta_H}{L} \approx 5 Re_L^{-1/2}, \quad \frac{\delta_T}{\delta_H} \approx Pr^{-1/3} \quad (30)$$

The computational domain should have  $H$  greater than the larger of  $\delta_H/L$  and  $\delta_T/L$ . In the code  $H$  was set at twice the maximum BL thickness predicted at the outflow.



The bottom surface consists of a streamline, for which the stream function can be arbitrarily set to a constant;

$$\psi_{i,0} = 0 \quad (31)$$

The conditions along the bottom for  $\omega$  and  $T$  surface depend on whether  $x$  corresponds to the starting region or the surface. Denote the coordinate of the surface leading edge as  $j_s$ :

$$j_s = \frac{X_s}{\Delta x}$$

and the conditions are (from Bejan)

$$\left. \begin{aligned} \omega_{i,0} &= -2 \frac{\psi_{i,1} - \psi_{i,0} - \Delta y}{(\Delta y)^2} \\ T_{i,0} &= T_{i,1} \end{aligned} \right\} \quad j < j_s \quad (32)$$

$$\left. \begin{aligned} \omega_{i,0} &= \frac{7\psi_{i,0} - 8\psi_{i,1} + \psi_{i,2}}{2(\Delta y)^2} \\ T_{i,0} &= 1 \end{aligned} \right\} \quad j \geq j_s \quad (33)$$

On the inflow surface  $u = 1$ ,  $v = 0$ , so

$$\psi_{0,j} = j \Delta y \quad (34)$$

and

$$\omega_{0,j} = \frac{2\psi_{1,j} - \psi_{0,j} - \psi_{2,j}}{(\Delta y)^2} \quad (35)$$

$$T_{0,j} = 0 \quad (36)$$

For the top surface  $u = 1$  (and  $v \neq 0$ ); use a forward difference approximation to the derivative on  $\psi$  to get

$$\psi_{i,N_y} = \frac{2}{3} \left( \Delta y + 2\psi_{i,N_y-1} - \frac{1}{2}\psi_{i,N_y-2} \right) \quad (37)$$

With regard to the streamfunction, use the free stream condition in Bejan;

$$\omega_{i,N_y} = 2 \frac{\psi_{i,N_y} - \psi_{i,N_y-1} - \Delta y}{(\Delta y)^2} \quad (38)$$

$$T_{i,N_y} = 1 \quad (39)$$

Finally, the outflow conditions are

$$\psi_{N_x,j} = 2\psi_{N_x-1,j} - \psi_{N_x-2,j} \quad (40)$$

$$\omega_{N_x,j} = \omega_{N_x-1,j} \quad (41)$$

$$T_{N_x,j} = T_{N_x-1,j} \quad (42)$$

The *Mathematica* code which implements the solution is given in the appendix.

### 3.6.3 Calculation results

Shown in Fig. (5) are contour plots of stream function (top) and temperature contours (bottom) for a laminar boundary layer. The simulation corresponds to  $Re_L = 10^4$  and  $Pr = 1$ . The starting length was  $X_s = 0.1$ , and 40 and 80 mesh points were used in the vertical and horizontal directions. The contours correspond to a dimensionless time of 2. It will take the convective flow one unit of time to traverse the heated surface – this is because the time is scaled with the convective residence time  $L/U_\infty$  – and the results reach essentially

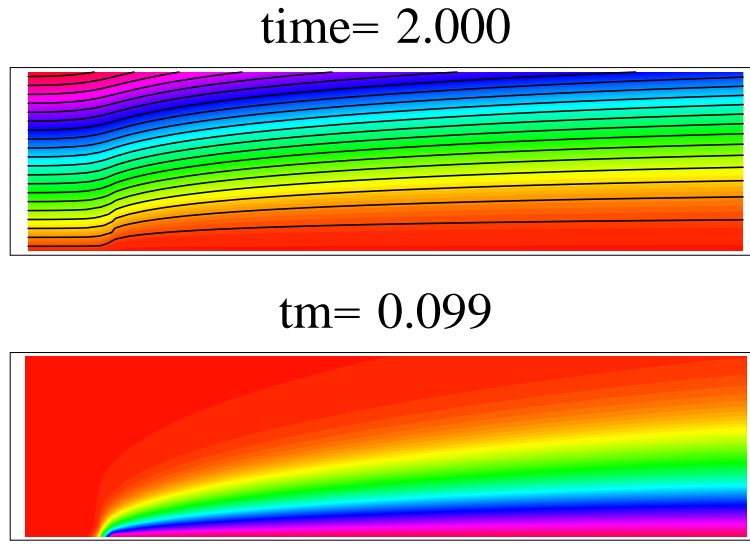


Figure 5: Stream function (top) and isotherms (bottom), laminar boundary layer,  $Re_L = 10^4$ ,  $Pr = 1$ .

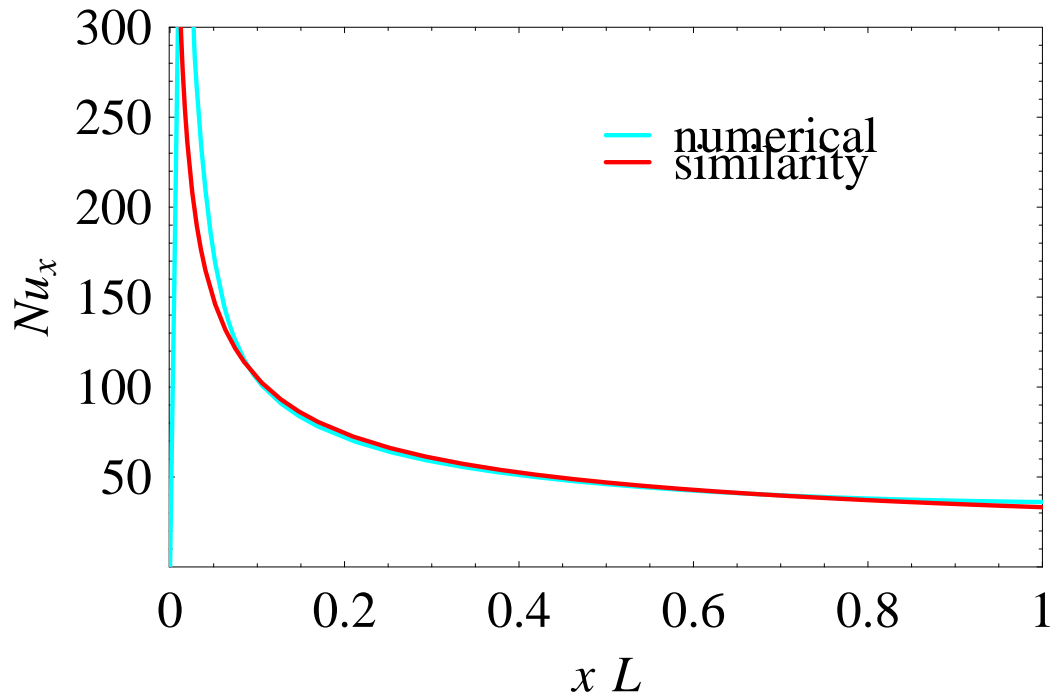


Figure 6: Numerical and analytical  $Nu_x$ ,  $Re_L = 10^4$ ,  $Pr = 1$ .

a steady state after this time span. The plot shows, as expected, a growing boundary layer thickness in the flow direction. Note also that the stream lines are not parallel to the upper surface; this illustrates the displacement effect discussed in the previous section.

A more quantitative measure can be obtained by calculating the local Nusselt number along the surface. The Nusselt number is the dimensionless temperature gradient; for our conditions it is

$$Nu_x = - \left. \frac{\partial T}{\partial y} \right|_0 \approx \frac{T_{i,0} - T_{i,1}}{\Delta y} \quad (43)$$

The results are shown in Fig. (6). For comparison, the analytical result obtained from the boundary layer approximation of

$$Nu_x = 0.332 Re_x^{1/2} Pr^{1/3} \quad (44)$$

is also shown, and the numerical and analytical results match almost perfectly at points sufficiently removed from the leading edge.

More results will be presented during the lecture...